

Test Report:
Single Event Effects Testing of ADC14155WG-MLS
Analog-to-Digital Converter (National Semiconductor).

Stephen Buchner, PSGS/NASA-GSFC
Melanie Berg, MEI/NASA-GSFC
Christina Seidleck, MEI/NASA-GSFC

6th May, 2009

1. Introduction

This report describes single event effects (SEEs) testing of the ADC14155 Analog-to-Digital Converter (ADC) from National Semiconductor. This device is a 14-bit ADC with a maximum sampling rate of 155 MSPS. The goal was to determine the SEE characteristics when the device was exposed to beams of heavy ions at an accelerator. SEEs observed during testing consisted of Single Event Transients (SETs) characterized by error bursts containing anywhere from a single error to hundreds of consecutive errors, and clock losses, that lasted for many clock cycles before recovering without any external intervention. As part of this test, SET data were collected for three different sampling modes (one-point, two-point and four-point) and the cross-section as a function of ion LET, error amplitude distributions and burst characteristics (number of bursts vs burst length) were compared.

2. Background

Over the years, various approaches have been used for testing ADCs for SEE sensitivity. The plethora of approaches is the result of an absence of a standardized test method that stipulates test conditions such as input amplitude and frequency and the sample rate. The absence of a standardized approach is due to the large number of possible applications for ADCs, so that, ideally, ADCs would be tested in the exact configurations in which they will be used. Such an approach is clearly impractical because of the cost involved in repeated SEE testing and the limited availability of accelerator beam time.

The simplest test involves the use of a DC input for which the output is a constant digital value and any deviations of the output during exposure to beams of heavy ions may be assumed to be due to SETs. In practice, however, there is noise in the system, which means that only those transients with amplitudes greater than the noise are counted. To avoid having to collect and analyze an overwhelming amount of data, a window in software is established that brackets the noise around the expected digital output and only those signals outside the window are counted. The problem with this approach is that the SET sensitivity has, in some cases, been shown to vary with input. A better test would be one that included measurements over the full input voltage range, requiring a large number of SEE tests at a variety of DC input voltages. Because of the considerable testing time required for this approach, it is best avoided. Furthermore, in many applications the input is dynamic rather than static, and it is best to test using a setup as close to the intended application as possible.

SET testing with dynamic inputs should give a more accurate picture of the device's SET sensitivity. This can be accomplished by applying a slowly varying input voltage, such as a linear ramp or a sine wave, and using a sampling rate much faster than the signal frequency. This method allows the full range of input voltages to be tested for SET sensitivity. However, it is generally desirable to use a high-frequency input signal because SEE rates generally increase with frequency.

We report here on the use of three different methods of sampling the data for the ADC14155 - one-point, two-point, and four-point. The four-point method samples the data at four times the signal frequency, whereas the two-point method samples at just

over once per clock cycle, and the one-point method, samples the data just once per clock cycle.

3. Measurement Approach

The approach taken for this experiment was to compare the SETs (transients and clock losses) for various sampling methods: 1-point, 2-point and 4-point. The input was a sine wave with peak-to-peak amplitude of approximately 1 V. The input range is adjustable in hardware, and was set to 2 V, so that the sine wave covered approximately half of the input range. A brief description of the three sampling methods follows:

a. *Single-Point Measurement*

For the single-point approach, the clock and input have the same frequency and the input is sampled once every clock cycle. As a result, the point on the sine wave at which the signal is read does not change and the digital output has the same value for each reading. During our tests we did not vary the phase between the signal and the clock in order to vary the point along the curve where sampling took place. Due to noise, the output fluctuates about the expected value. SETs manifest themselves as deviations from the expected digital output value. Before the part is exposed to the ion beam, a series of readings is taken to establish the average value and the magnitude of the noise. Using software, a window is defined that brackets the expected output as well as the noise. During exposure to the ion beam, a reading outside the window signifies the presence of an SET. Fig. 1 illustrates the technique.

Measurements were taken with the clock and input signal tied together and the frequency set at either 100 MHz or 10 MHz. The purpose was to uncover frequency-dependent effects in the SET cross-section. It is also important to note that this approach, which gives a constant output reading because the sine wave is sampled at the same relative location on the sine wave, is not the same as using a DC input. In the case of a dynamic input, some of the captured SETs will have been generated prior to the sampling time when the input voltage will differ from that when the signal is sampled. Varying the value at which the sine wave was read by adding a phase shift between the clock and the signal makes it possible to sample the sine wave at different amplitudes. There was not sufficient time available to do this. One concern is that the one-point method, in which sampling is done only once per clock cycle, might miss transients much shorter than one clock cycle.

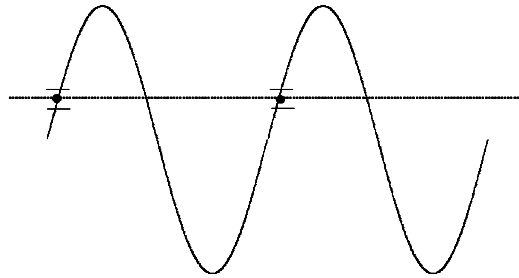


Fig. 1. Input sine wave showing the location of the sampling points. A window is defined in software around each point. The dashed line shows the constant value of the output. Only readings outside the window were counted as SETs.

b. Two-Point Measurement

In the two-point measurement, pioneered by Kruckmeyer et al [5], the clock frequency is set just a little faster than the input signal frequency. The requirement that two successive samples differ by just one LSB is given by:

$$f_{in} = f_s \left(1 - \frac{1}{2^N \pi}\right) \quad [1]$$

where f_s is the sampling frequency, f_{in} is the signal frequency and the amplitude is assumed to be half the full scale of 2^N . The main assumption in this calculation is that the input is a sine wave with the largest change around 0V. Using equation 1, for a clock (sampling) frequency of 100 MHz, the input should have a frequency of 99.99999241 MHz. However, in our experiments the input frequency was set to 99.98 MHz, which means that the difference was more than 1 bit, depending on where along the sine wave the readings were taken. A window of 96 units (6 lowest bits) was used for these measurements, i.e., an error (SET) was logged if the difference between the two points was greater than 96. Two additional limits were set, one just greater than the maximum and one just slightly more negative than the minimum. Readings beyond these two limits would also be counted as errors, regardless of their amplitudes. The maximum and minimum limits were set to include bursts of SETs in which the output was driven either to the maximum or minimum digital value and pinned there for many clock cycles. If only the differences were taken, these readings would not be registered as SETs because successive outputs would be less than the window.

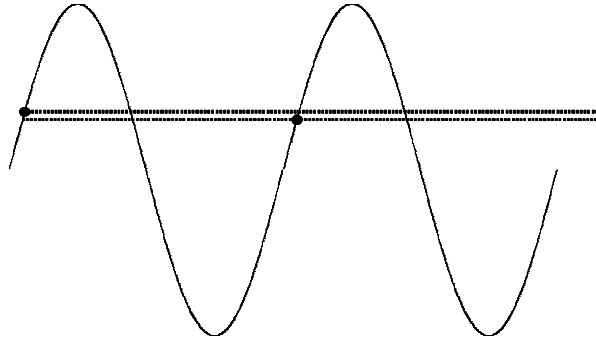


Fig. 2. Consecutive measurements are taken that differ by a small amount determined by the difference in frequency between the clock and the input. For the ADC14155, one measurement was done with a clock frequency of 100 MHz and a data input frequency of 99.98 MHz. These conditions lead to a difference of more than one LSB between consecutive measurements.

c. Four-Point Measurement

The four-point method involves setting the clock frequency to four times the analog input signal frequency. Therefore, for a sampling frequency of 100 MHz, the input frequency is set at 25 MHz. Prior to the irradiation, the amplitudes at the four points were measured hundreds of times and the averages taken to obtain the expected values. Because of system noise, each of the data points was bracketed by a window of 176 (7 LSBs). When an error was detected at any of the points, the values of all four were recorded. The usefulness of this approach is that it samples the sine wave at four

different points instead of just one. That is an improvement over the single-point method because the four points were sampled at different amplitudes, making the method potentially more sensitive, and it is also more likely that an SET shorter than the sampling period would be captured.

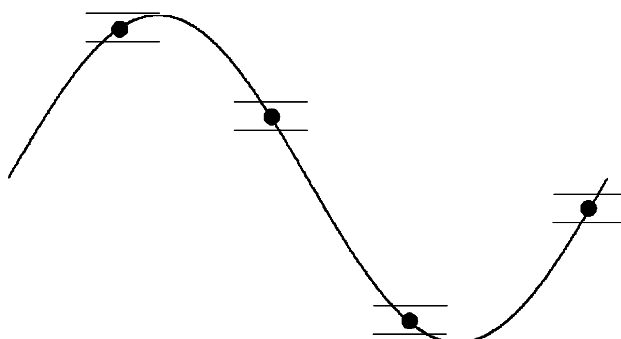


Fig. 3. Input signal (sine wave) and the four points at which measurements are made. The windows are set based on the noise levels prior to onset of irradiation. The clock signal was four times as fast as the analog input signal.

4. Experimental Approach

The part was manufactured by National Semiconductor (NS) and is designated as the ADC14155WG-MLS (<http://cache.national.com/ds/DC/ADC14155QML.pdf>). Testing was conducted in June 2008 at Texas A&M Cyclotron Institute using the 25 MeV/amu beam. The ADC14155 was mounted on an evaluation board manufactured by NS (http://national.com/appinfo/adc/files/ADC14155UsersGuide_r0p0.pdf) and modified by replacing their standard connector with a micro-strip connector to make it compatible with NASA's LCTS board. Another modification was the removal of the output level shifter.

The NASA-GSFC Radiation Effects and Analysis Group's Low Cost Test System (LCTS) was used to control the operation of the ADC during testing. Both the clock and input signals (sine waves) were supplied by an external generator (Tektronix Dual Wave Form Generator – AFG3252). They were locked together so that their phase difference remained constant throughout a run. On every clock cycle, a signal appeared at DRY (data ready) to signal the FIFO to prepare to accept data. During clock losses, the external clock still supplied a signal to the DUT, but no signal appeared at DRY. When a transient was flagged, the reading and the time stamp were transferred to the LCTS board and stored on the computer. Scripts were written to convert the data, which were in two's complement (allowing for negative numbers), into readable form. The data were then analyzed using a software program that could distinguish clock losses from bursts of errors and single errors.

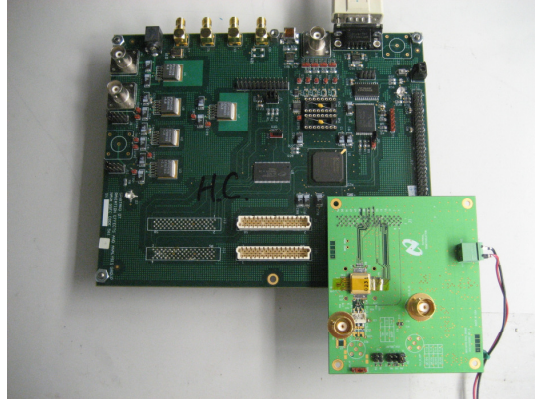


Fig. 4. The evaluation board (right bottom) was supplied by National Semiconductor. The ADC14155 DUT is located half-way down from the top and just to the left of center. The other board is the low-cost test board that interfaces to the computer and is used for controlling the ADC14155.

The input signal range is specified in the data sheet as 2.6 V. We used a 1 V peak-to-peak (-0.5V to +0.5V) signal. A 14-bit ADC has 16,384 different readings and the values go from -8,192 to +8191. Dividing the range (2.6V) by the number of bits (16,384) gives a voltage resolution of 1.5869×10^{-4} volts, or, approximately, 159 μ V.

Fig. 4 shows a picture of the motherboard and daughterboard electrically connected via a special microstrip connector. The two boards were mounted in a vice on an X-Y-Z- θ table in front of the exit beam of the accelerator. Long cables were connected to the low-cost test board so that the device could be operated remotely from the experimental control room.

Table 1 shows the ions, their energies, LETs and ranges used for testing the ADC14155. In addition, data were also taken at 45 degrees to the normal, which increase the LET by a factor of 1.41.

Table I
Ions used at TAMU

Ion	Energy (MeV)	LET (MeV.cm²/mg)	Range (μm)
Ne	523	1.8	799
Kr	1821	20.9	493
Xe	2645	41.5	332

5. Experimental Results

a. One-point Method

Ion-beam testing for the one-point sampling method was conducted using both 100 MHz and 10 MHz. However, the data presented here for the one-point method will be for 100 MHz as the data characteristics at both frequencies are fundamentally the same. SETs occurred across the entire LET spectrum – from 1.8 to 58.69 MeV.cm²/mg.

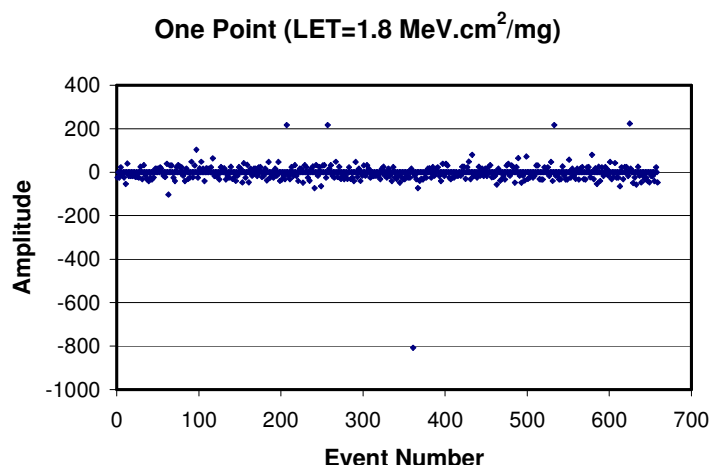


Fig. 5. SET amplitude deviation from expected value for all SETs measured at an LET of 1.8 MeV.cm²/mg using the single-point sampling approach at 100 MHz. (Run86).

Fig. 5 shows all the SET amplitudes (difference between measured value and expected value) when the device was exposed to ions with a LET of 1.8 MeV.cm²/mg. Only those SETs that deviated in the positive or negative directions from the expected value by more than 16 were captured. Captured SETs had both positive and negative amplitudes. Most of the events consisted of single transients – those that lasted less than a clock cycle – but there were three bursts, each of length two clock cycles. There were no clock losses. Most of the SETs had amplitudes under 100 units (15.8 mV), but there were a few with amplitudes of 200 units (31.6 mV) and above.

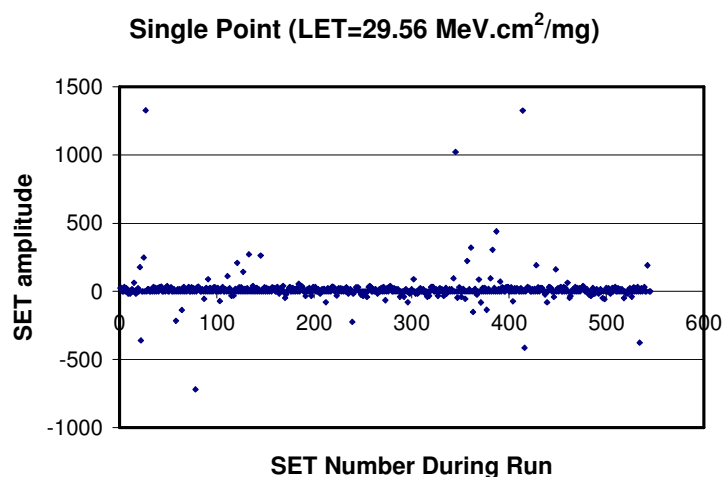


Fig. 6. SET amplitudes (deviation from expected value) for all the errors during run 40 (1-point, LET=29.6 MeV.cm²/mg, 100 MHz, Run40).

Fig. 6 shows the amplitudes of all the transients (whether in a burst or not) for a single run at a LET of 29.6 MeV.cm²/mg. Most of the events were in the form of single transients with a few bursts containing up to four consecutive transients. The expected value was 5424. The figures shows SETs with amplitudes up to about 1400

units greater than the expected value of 5424. There were no clock losses. Fig. 7 shows the distribution of errors among single SETs and bursts of SETs.

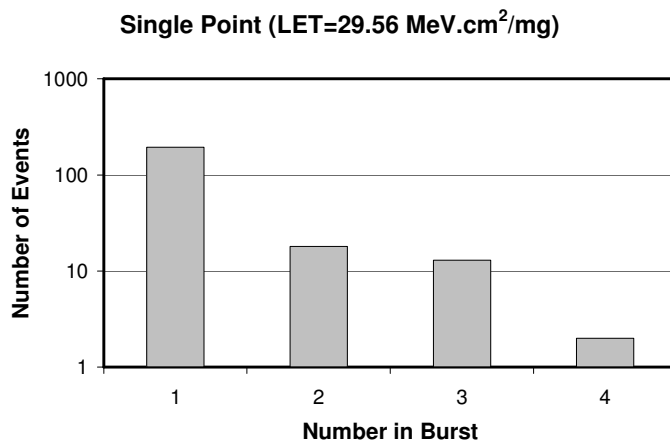


Fig. 7. Number of burst events as a function of number of SETs in a burst for LET = 29.56 MeV.cm²/mg at 100 MHz.

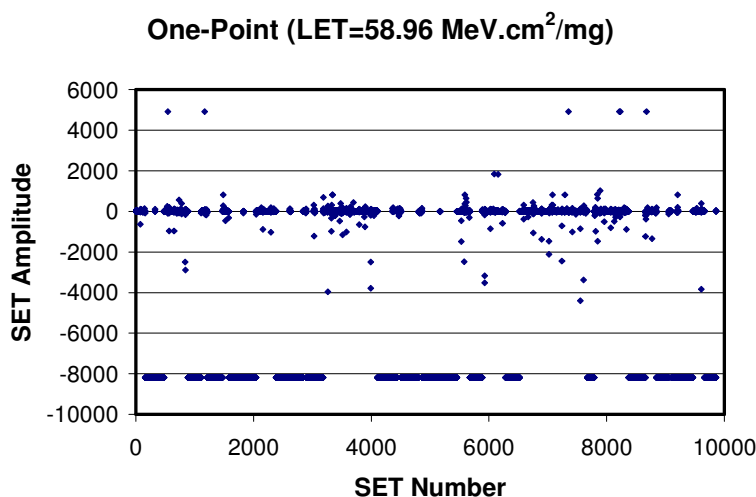


Fig. 8. Error amplitudes for all SETs captured during run 34 at a LET of 58.69 MeV.cm²/mg. The expected value was 3272.

Fig. 8 shows the SET amplitudes for Run 34, for which the LET was a maximum (58.69 MeV.cm²/mg) and the frequency was 100 MHz. The figure clearly shows that there are significantly more large negative-amplitude SETs than SETs with positive amplitudes. It appears that the largest negative amplitudes are about -8200. Since the expected value was 3272 and the negative amplitude was -8200, the maximum negative value at which the output gets pinned is about -4970.

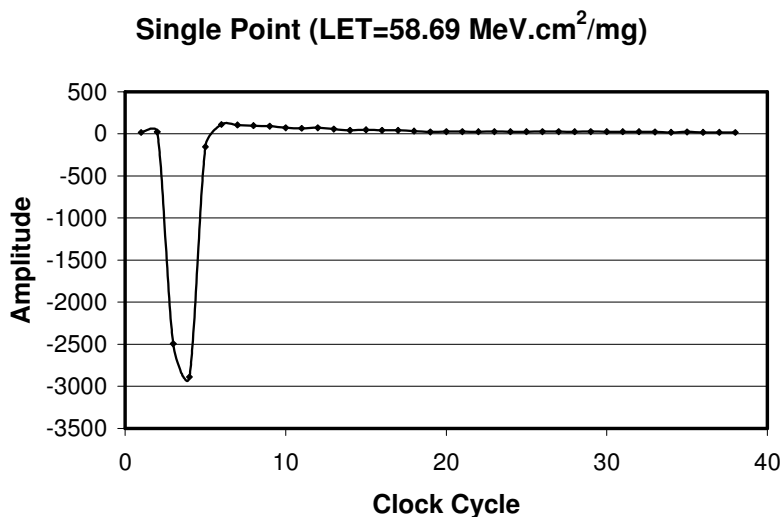


Fig. 9. An example of a single burst of SETs showing amplitude as a function of time. (Run 34).

Fig. 9 shows an example of the evolution over time of a single error burst. The burst has a large negative component that persists for only a few clock cycles. This is followed by a small but much longer positive component. The total duration of the burst is 38 clock cycles, or 380 ps for a 100 MHz clock. (The one-point sampling method is incapable of showing how the whole sine wave is distorted as it is only sampling a single point.)

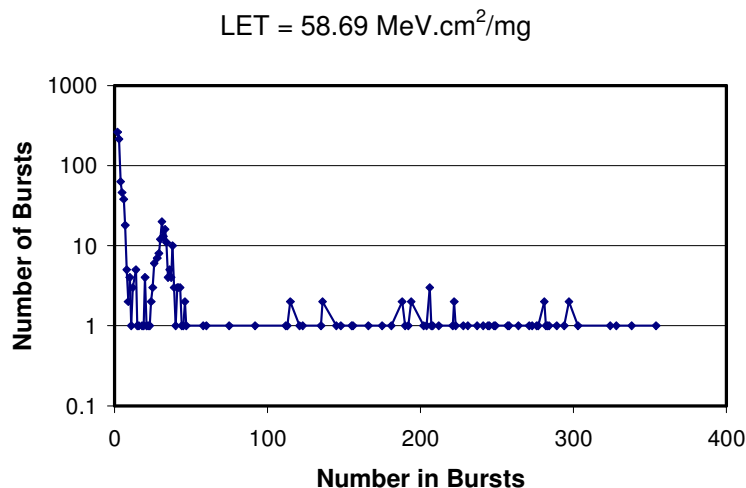


Fig. 10. Number of bursts as a function of the number of events in a burst for the one-point method at an LET of 58.96 MeV.cm²/mg and a frequency of 100 MHz.

Fig. 10 shows the distribution of burst lengths, i.e., the number of bursts containing a specific number of transients. (The y-axis has a logarithmic scale in order to make all points clearly visible). Comparison of the burst distribution shown in Fig. 10 with that in Fig. 7 clearly illustrates how much longer the bursts are at higher LETs. This evolution of burst length as a function of ion LET is shown in Fig. 11. The fact that the bursts are longer for higher LETs is not surprising. However, the odd shape of the

distribution, which has a peak at about 30 clock cycles, is unexpected and of unknown origin.

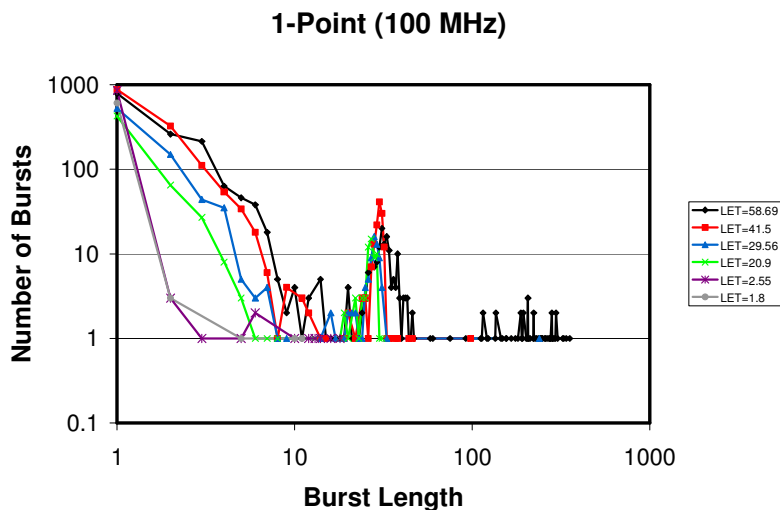


Fig. 11. Summary of number of bursts as a function of burst length (clock cycles) for different LETs and at a frequency of 100 MHz.

Fig. 12 shows the SET cross-section as a function of LET for the single-point measurement mode. In this plot, clock losses were ignored and only bursts were counted. Each burst contained anywhere from one transient to hundreds of transients. A burst was identified by the time-stamp as the transients within the burst were separated in time by a single clock cycle. The figure clearly shows that the SET cross-section increases linearly with LET and shows no sign of saturating. Also, the cross-section at 100 MHz is greater than at 10 MHz by a factor of 1.2. The increase in cross-section with frequency is not unexpected. However, the increase is not linear with frequency as is the case with combinational logic.

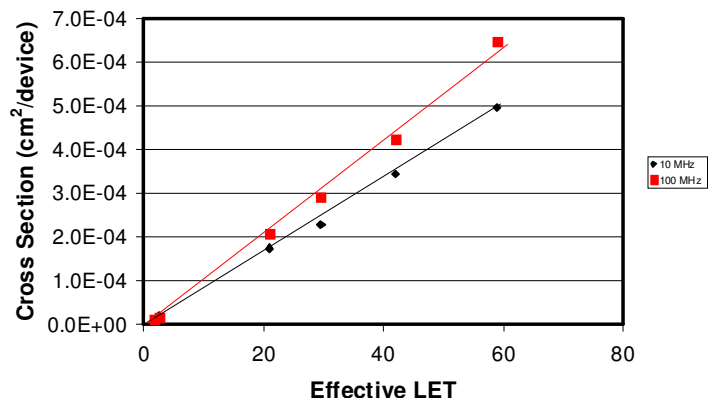


Fig. 12. SET cross-section as a function of ion LET for the one point method. The straight lines are approximate fits used to guide the eye.

Fig. 13 shows the SET cross-section as a function of ion LET for different windows around the expected output for SETs that include singles and bursts, but not

clock losses. As the window increases, the cross-section decreases. Fig. 13 clearly shows that the cross-section continues to increase above a LET of $58.69 \text{ MeV.cm}^2/\text{mg}$, with no hint of saturation. This makes it difficult to calculate error rates for which the saturated cross-section at high LETs is needed.

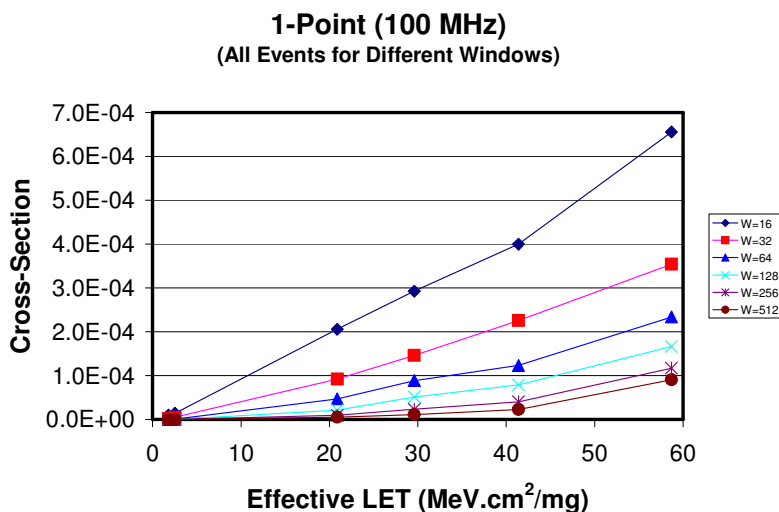


Fig. 13. Cross-section for all events (bursts and clock losses) as a function of LET for different time windows.

Clock losses for the one-point method occur at LETs of $42 \text{ MeV.cm}^2/\text{mg}$ and above. Fig. 14 shows the cross-section as a function of ion LET. Clock losses may be distinguished from bursts in that no data appear for a string of consecutive clock signals, whereas a burst is identified by the appearance of data for a string of consecutive clock signals. Note that the Clock-Loss cross-section increases significantly with frequency at the higher LET and has almost no effect at the lower LET. We have no explanation for this.

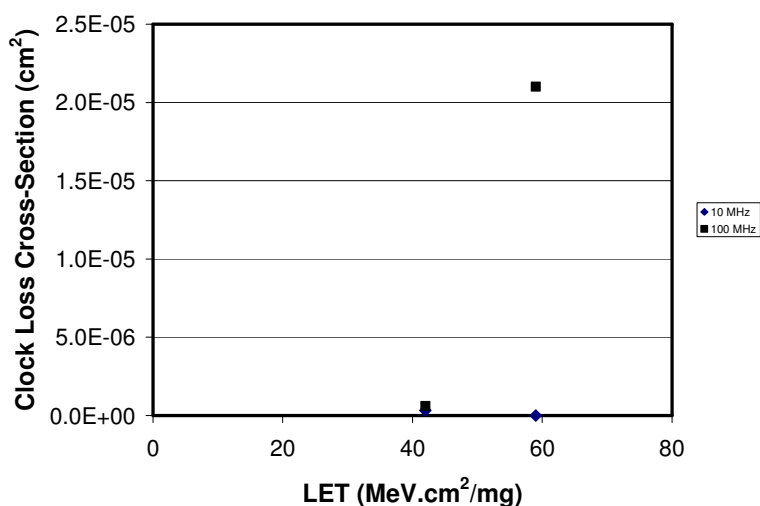


Fig. 14. Cross-section as a function of ion LET for clock losses at two different frequencies for one-point measurements.

b. Two-point Method

For the two-point method, the window was set at 96. Fig. 15 shows the amplitudes for all the SETs at LET = 2.546 MeV.cm²/mg and frequency = 10 MHz (Runs 67, 68, 69). All SETs were either singles or doubles. One would expect that, for errors in the two-point method in which differences between successive readings are taken, there should be at least two transitions for every event, i.e., the initial disturbance and the return. Fig. 15 shows that doubles always contains one positive and one negative component. Singles occasionally occurred when the initial deviation exceeded the preset window (96) by just a small amount, but the return did not, due to a change in the expected signal level or to changes in noise. Most of the transients had amplitudes that were smaller than 200 units, but a few were as high as 920.

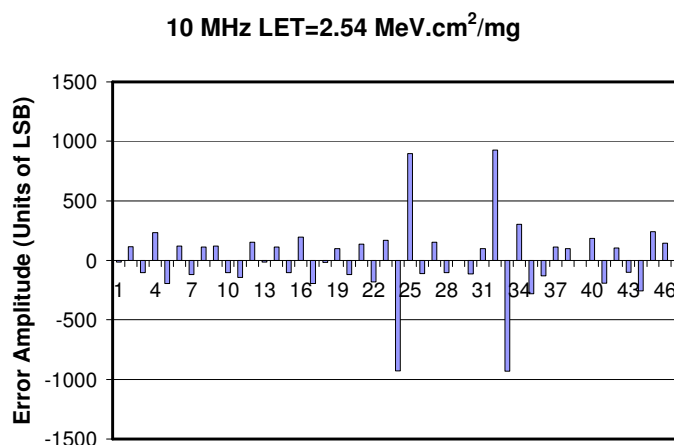


Fig. 15. Plot of all the amplitudes of the SETs captured during Run 69 for a LET of 2.546 MeV.cm²/mg and a frequency of 10 MHz.

At LET = 20.9 MeV.cm²/mg, many more SETs appear, some with amplitudes of about 8,000. Fig. 16 shows the amplitudes of all the transients from Runs 62 and 63 for a total fluence = 1x10⁷ particles/cm².

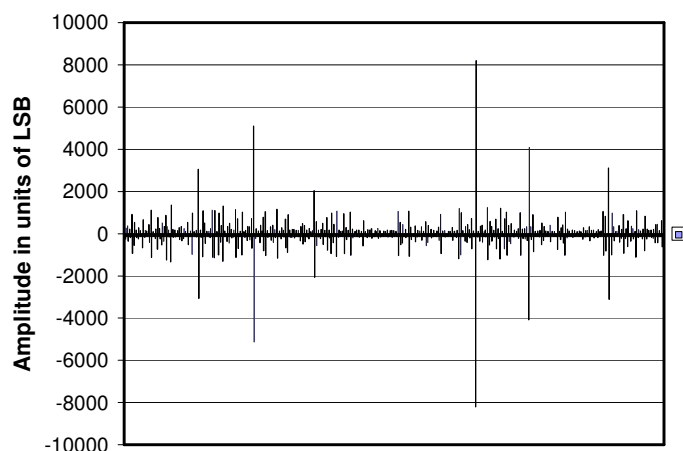


Fig. 16. SET amplitudes for all SETs for an LET of 20.9 MeV.cm²/mg and with a clock frequency of 10 MHz (Run 62 and 63).

Fig. 17 shows that for $\text{LET} = 41.5 \text{ MeV.cm}^2/\text{mg}$ and clock frequency = 10 MHz, there were both long and short error bursts. After error number 10, there is a long burst containing errors with small amplitudes that lasts for about 200 clock cycles. The errors have amplitudes less than that of the window (96). The explanation for this is that two additional levels were set, one at 7423, which is just larger than the maximum amplitude of the sine wave and one at -7375, which is just smaller than the minimum. Any SETs that are greater than the maximum or more negative than the minimum are automatically counted as SETs, independent of the difference. For this burst, the amplitude was more negative than -7375 and stayed there for almost 200 conversions. (This shows the importance of setting limits for the amplitudes that are driven to the positive or negative extremes.) Following the end of the long SET, the normal short SETs resume, some with amplitudes up to more than 8,000. Similar results were observed for LETs of $58.69 \text{ MeV.cm}^2/\text{mg}$.

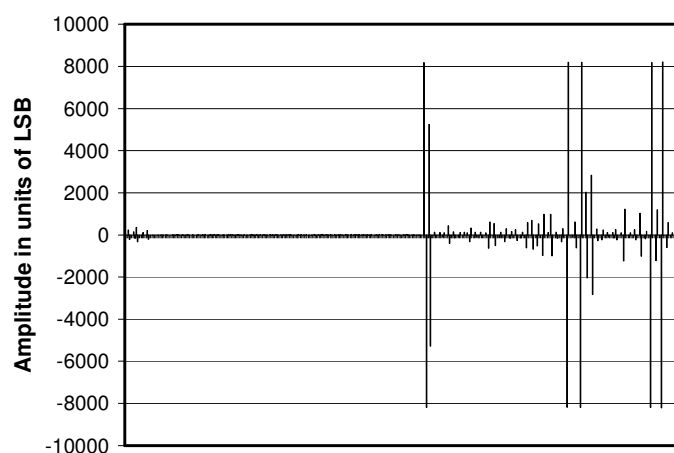


Fig. 17. SET amplitudes for an LET of $41.5 \text{ MeV.cm}^2/\text{mg}$ and a clock frequency of 10 MHz (Run 13).

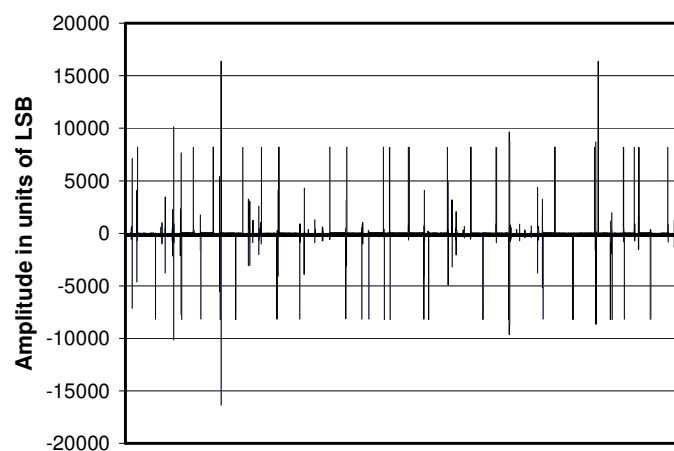


Fig. 18. Error amplitudes for an LET of $58.7 \text{ MeV.cm}^2/\text{mg}$ and a frequency of 100 MHz. There are numerous transients that appear to have amplitudes smaller than the window of 96 but they actually have large amplitudes and are parts of long bursts outside the maximum and minimum limits.

Fig. 18 shows that at high LETs there are numerous transients with large amplitudes as well as many clock losses. Since the window is set at 96, amplitudes smaller than 96 are due to transients that have exceeded the two limits, and are also part of a longer burst, where the differences between successive transients in the burst are smaller than the window. There are also clock losses for which the amplitudes are 0.

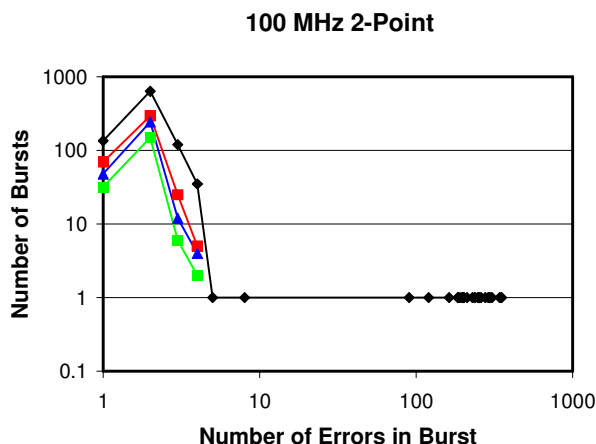


Fig. 19. Number of bursts as a function of number of errors in a burst for different values of LET.

Fig. 19 is a plot of the number of bursts that have a specific number of errors in the burst. Since the fluences were not all the same for the different LETs, the number of bursts were scaled by their fluences. The figure clearly shows that the bursts are all below 10 clock cycles long (10^{-7} seconds) except for the highest LET of 58.7 MeV.cm²/mg, and that the higher the LET the longer the burst and the greater their number. Since every burst in the two-point method should consist of at least two errors (one for the initial displacement and the second for the return), the fact that there are bursts with just one error is attributable to a combination of noise and a changing base line such that the return is less than window, and is therefore not recorded.

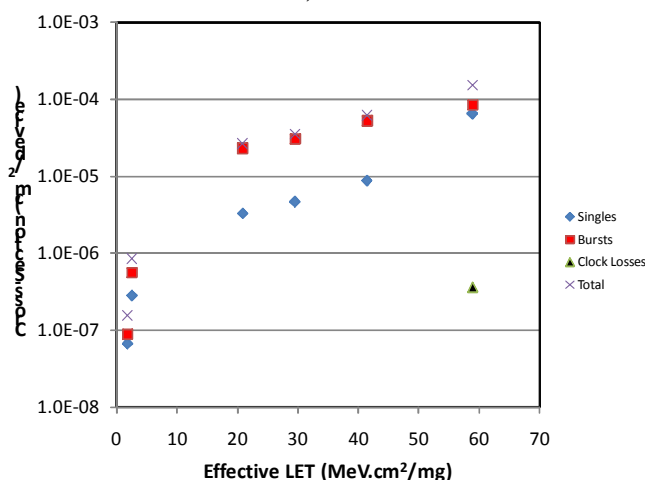


Fig. 20. Cross-section (at 10 MHz) as a function of effective LET for singles errors, bursts of errors, clock losses and the total using the two point method.

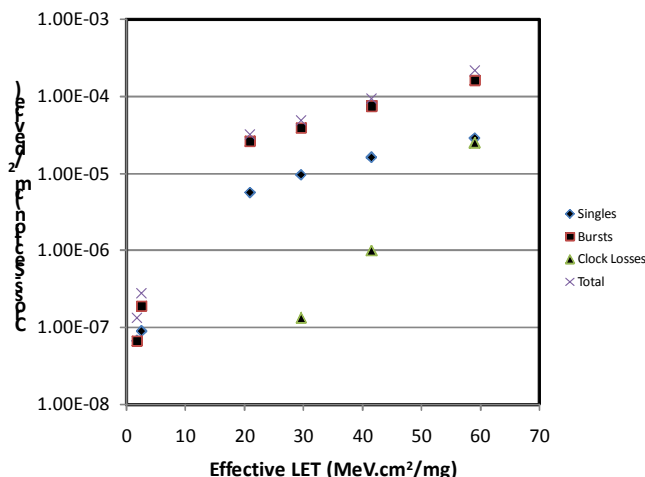


Fig. 21. Cross-section (at 100 MHz) as a function of effective LET for singles errors, bursts of errors, clock losses and the total using the two point method.

Figs 20 and 21 show the cross-sections as a function of effective LET for singles, bursts, clock losses and the total of all events. There is no indication of saturation and there are very few differences between the data for 10 MHz and 100 MHz.

c. Four-point Method

The four-point method requires that the sampling signal (clock) be set to a frequency four times that of the input signal. In these measurements, the sampling frequency was 100 MHz and the input signal frequency was 25 MHz. The windows around the expected values were set at 176 units, which is equivalent to the 7 least significant bits. This value is much greater than for the one-point measurement (16) because two of the four points being measured (see Fig. 22) are close to the steepest part of the curve where small amounts of jitter (noise) in the clock can lead to relatively large variations in the output.

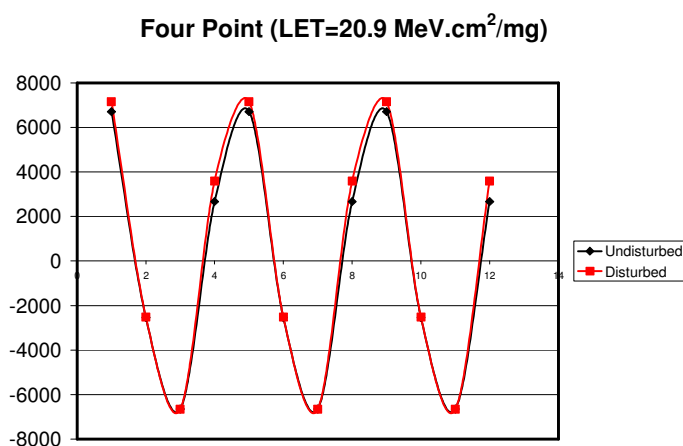


Fig. 22. Plots of the disturbed and undisturbed sine waves for the four-point method at an LET = 20.9 MeV.cm²/mg and a clock frequency of 100 MHz.

Fig. 22 shows a typical SET for a LET of $20.9 \text{ MeV.cm}^2/\text{mg}$. The figure needs some explanation. First, the four data points are repeated three times. Drawing the curve through only four points leads to distortions at the ends. The two curves that are defined by points 5, 6, 7, and 8 are the ones that most closely approximate those of the input signal and the disturbed signal. Second, a smooth curve is drawn through all the points using the XY (scatter) plot option in Excel. The fit fails to reproduce the exact shape and amplitude of the signals because there are only four data points. However, it is helpful for visualizing the ion-induced changes in the curves. Fig. 22 shows that the output signal is only slightly altered by the ion strike.

The fact that the above SET has points 1 and 3 outside the window and points 2 and 4 inside the window confirms that the distortion induced by the single event is small. That particular SET is part of a single long burst of more than 2000 consecutive SETs, all very similar in shape. Fig. 23 shows a plot of all four points for all the transients in that long burst. The data show that for every one of the more than 2000 SETs, points 1 and 3 are outside the window, whereas points 2 and 4 are inside the window. The amplitudes appear to increase gradually over time, the cause of which is unknown. It took the system over 8000 (4 per SET) clock cycles to recover. For a clock of 100 MHz, the time during which the burst lasted was about $80 \mu\text{s}$ ($8000 \text{ clock cycles} \times 10^{-8} \text{ s per clock cycle}$.)

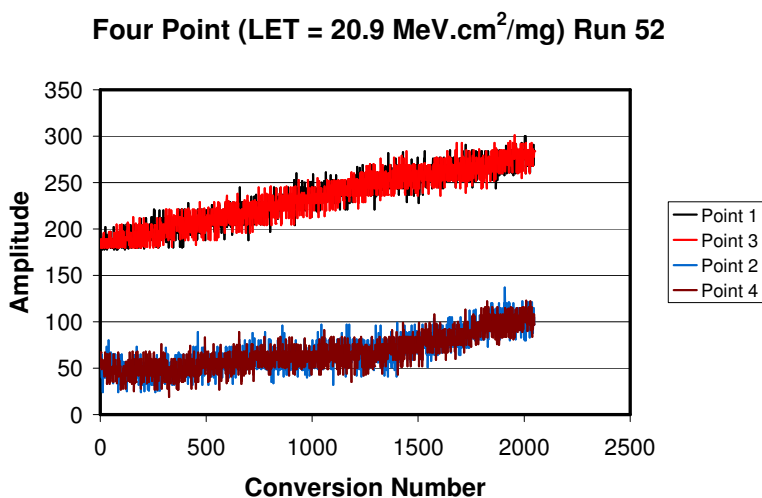


Fig. 23. Amplitudes (deviations from the expected values) of the four points in a single long burst. All the SETs have points 1 and 3 outside the window, whereas points 2 and 4 are inside that window. The window was set to 176 units.

Figs. 24 shows that at a higher LET ($29.56 \text{ MeV.cm}^2/\text{mg}$), the sine waves are more distorted by the transients, with all four points outside the window (176 units), leading to a significant reduction in amplitude. The figure shows the first three cycles of a burst of 39 consecutive distorted sine wave transients that together form a single burst. (The plot is different from that of Fig. 22 because the first four points are not repeated.) The undisturbed sine wave is included in the figure to show how large the deviation is for ions with higher LETs. Figs. 24-27 show additional examples of SETs at the same LET that have much greater deviations.

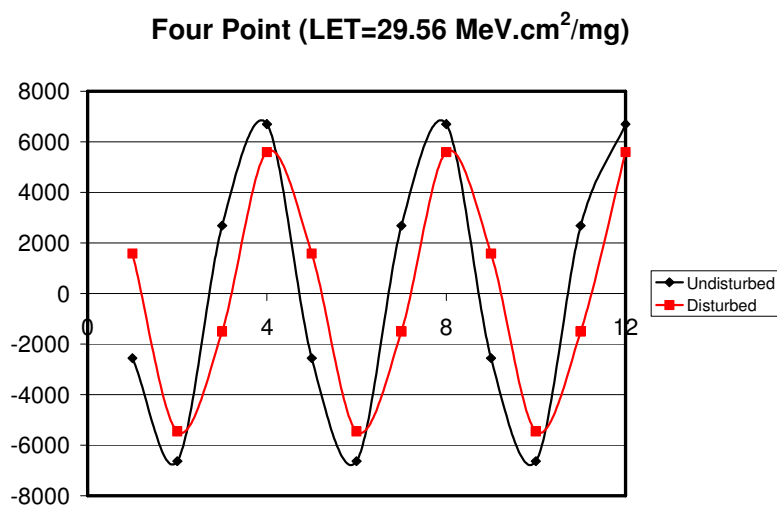


Fig. 24. Example of a transient for a LET of 29.56 MeV.cm²/mg. All four points were outside the window, and the resulting SET amplitude was smaller than that of the undisturbed sine wave. (Run 53).

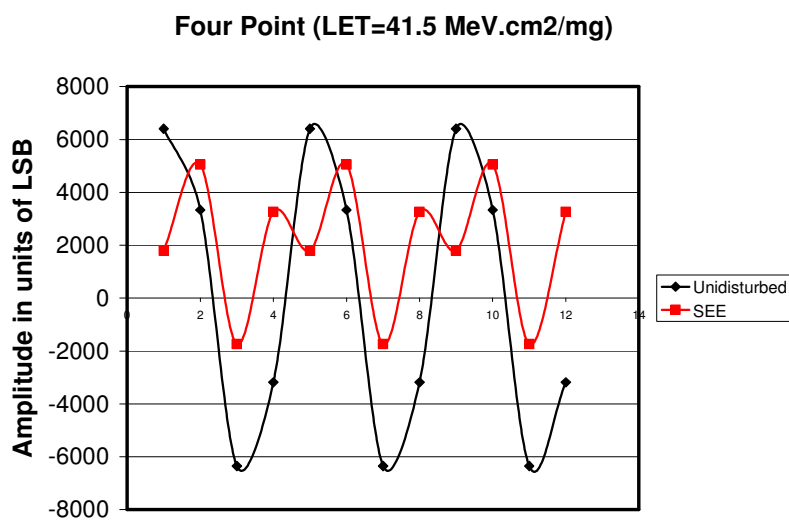


Fig. 25. Example of a transient for a LET of 29.56 MeV.cm²/mg. All four points were outside the window, and the resulting SET amplitude was smaller than that of the undisturbed sine wave. (Run 53).

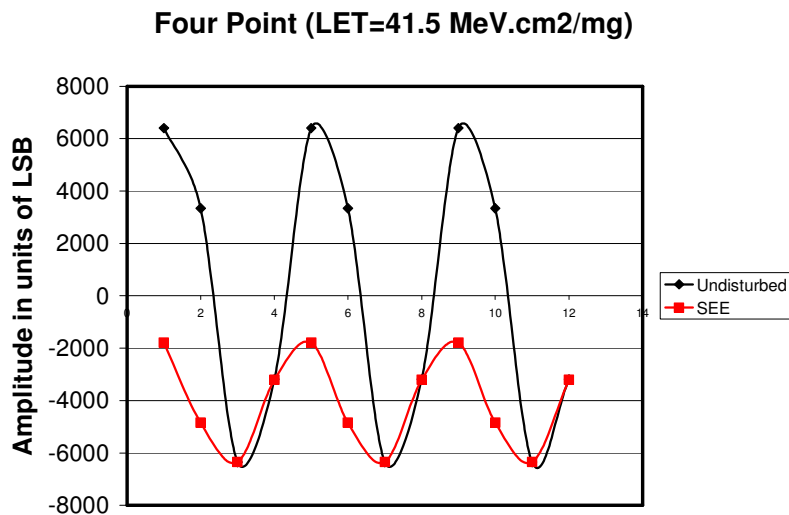


Fig. 26. Example of a transient for a LET of 29.56 MeV.cm²/mg. All four points were outside the window, and the resulting SET amplitude was smaller than that of the undisturbed sine wave. (Run 53).

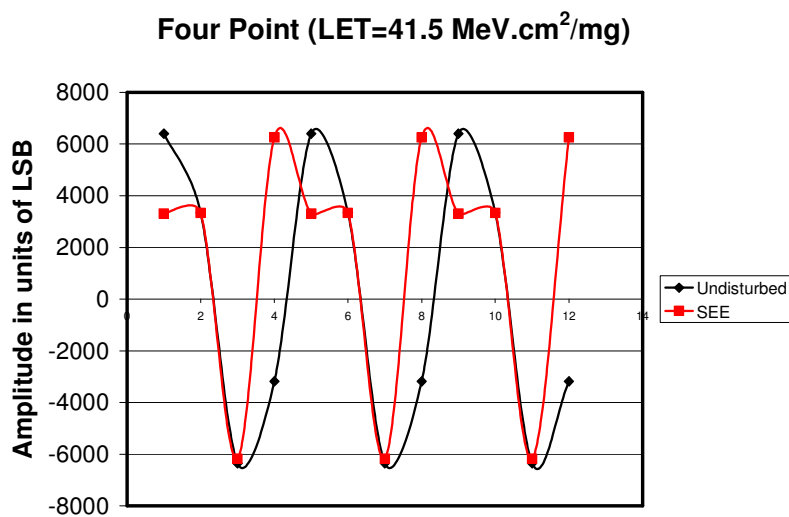


Fig. 27. Example of a transient for a LET of 29.56 MeV.cm²/mg. All four points were outside the window, and the resulting SET amplitude was smaller than that of the undisturbed sine wave. (Run 53).

SETs with similar characteristics are seen at even higher LETs. Figs. 28 and 29 are examples of how the SETs manifest themselves. The characteristic shapes are very similar to those at lower LETs. The primary difference at higher LETs is the presence of clock losses, which are totally absent at lower LETs.

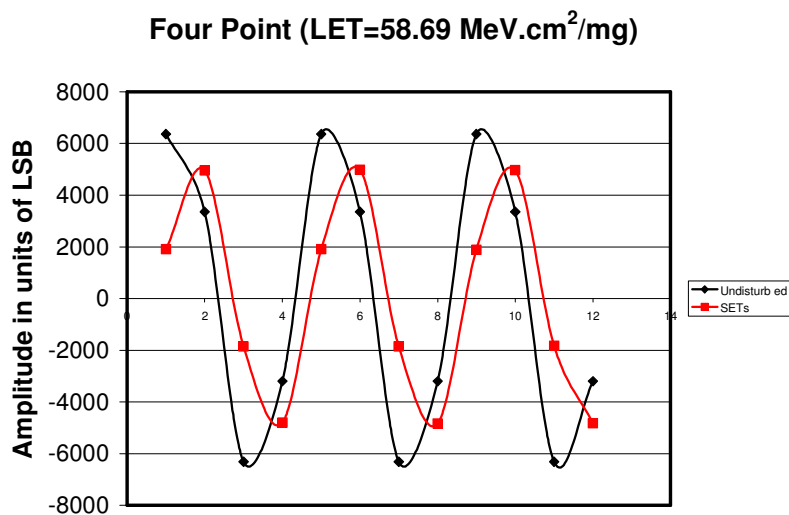


Fig. 28. Example of a transient for a LET of 58.69 MeV.cm²/mg. All four points were outside the window, and the resulting SET amplitude was smaller than that of the undisturbed sine wave. (Run 18).

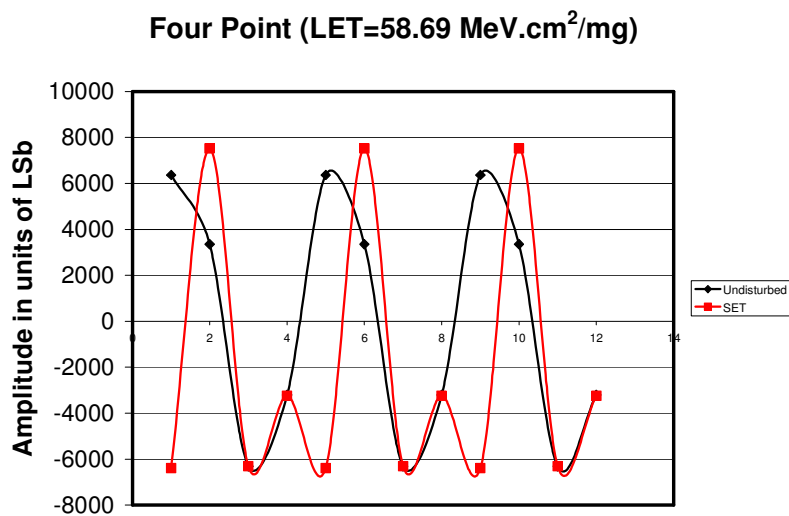


Fig. 29. Example of a transient for a LET of 58.69 MeV.cm²/mg. All four points were outside the window, and the resulting SET amplitude was smaller than that of the undisturbed sine wave. (Run 18).

Fig. 29 shows how the four-point method is superior to the one-point method as far as capturing SETs is concerned. The figure shows the presence of large deviations from the expected values for points 5 and 6 but not for points 7 and 8. If the voltage at which the SET was sampled in the one-point method were chosen to be that of either points 7 and 8 in Fig. 26, no SETs would have been registered. The presence of additional points increases the likelihood of detecting SETs.

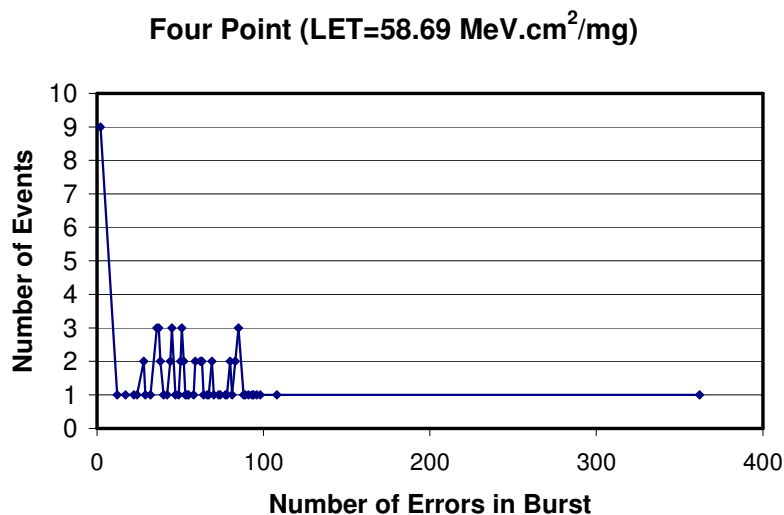


Fig. 30. Number of burst events as a function of the number of SETs (errors) in the burst for an LET of 58.69 MeV.cm²/mg.

Fig. 30 shows the number of burst events as a function of the number of errors in a burst. The figure shows 9 bursts with just a single error and then the number drops rapidly for bursts with more errors. Most of the bursts have fewer than 100 errors but there was one that consisted of almost 400 consecutive SETs.

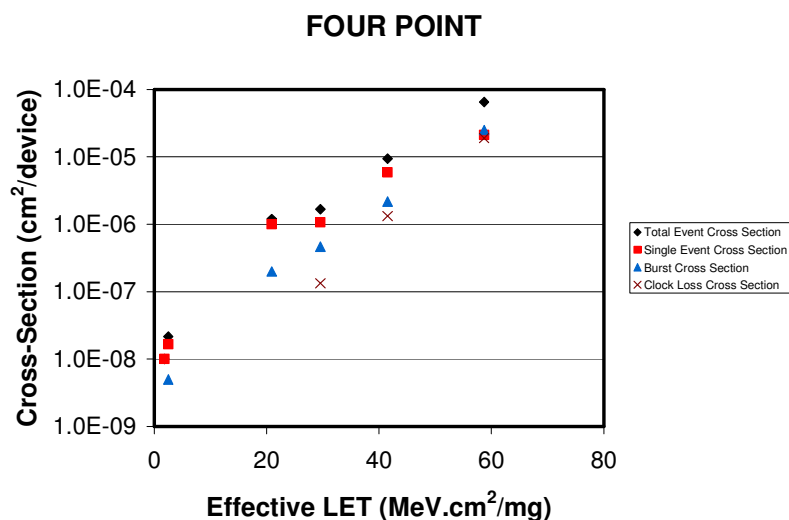


Fig. 31. SET cross-section as a function of effective LET for four-point measurements for singles, bursts, clock losses and the sum of all events.

Fig. 31 shows the SET cross-section as a function of effective LET for single SETs, bursts of SETs and clock losses as well as their sum. As in the case of the single-point measurements, the cross-section shows no indication of saturation, making the error rate calculation difficult. The threshold LET is below 1.8 MeV.cm²/mg.

6. Summary

1. The SET response of the ADC14155 consists of:
 - a. Bursts of transients.
 - b. Temporary clock losses that recover on their own.
 - c. A possible SEFI (observed only once at a LET=58.96 MeV.cm²/mg in the 4-point method).
2. At low LETs, the SETs consist primarily of bursts of errors. As the LET increases, so do the number of bursts per unit fluence, the amplitudes of the individual transients in a burst, and the number of transients in a burst.
3. At high LETs some of the bursts lasted hundreds of clock cycles.
4. At high LETs, clock losses were observed that lasted for many clock cycles but in all cases, except one, normal operation recovered without intervention.
5. The SET rate increased with sampling frequency in the one point method, and barely in the two-point method.